Hydrogen Evolution

Deutsche Ausgabe: DOI: 10.1002/ange.201602543
Internationale Ausgabe: DOI: 10.1002/anie.201602543

Enhanced Photoexcited Carrier Separation in Oxygen-Doped $ZnIn_2S_4$ Nanosheets for Hydrogen Evolution

Wenlong Yang[+], Lei Zhang[+], Junfeng Xie, Xiaodong Zhang, Qinghua Liu, Tao Yao,* Shiqiang Wei, Qun Zhang, and Yi Xie**

Abstract: *Limited by the relatively sluggish charge-carrier separation in semiconductors, the photocatalytic performance is still far below what is expected. Herein, a model of $ZnIn_2S_4$ (ZIS) nanosheets with oxygen doping is put forward to obtain in-depth understanding of the role that doping atoms play in photocatalysis. It shows enhanced photocatalytic activity compared with pristine ZIS. The electron dynamics analyzed by ultrafast transient absorption spectroscopy reveals that the average recovery lifetime of photoexcited electrons is increased by 1.53 times upon oxygen incorporation into the ZIS crystals, indicating enhanced separation of photoexcited carriers in oxygen-doped ZIS nanosheets. As expected, the oxygen-doped ZIS nanosheets show a remarkably improved photocatalytic activity with a hydrogen evolution rate of up to 2120 $\mu mol\, h^{-1} g^{-1}$ under visible-light irradiation, which is 4.5 times higher than that of the pristine ZIS nanosheets.*

As a clean and efficient source of energy, hydrogen is receiving increasing attention because of its potential in solving the energy shortage arising from the overuse of fossil fuels and the resulting serious environmental pollution problems.[1] In the past decades, photocatalytic hydrogen evolution on semiconductors was considered to be a promising and efficient solution to convert inexhaustible solar energy into storable hydrogen.[2] Up to now, although a great variety of impressive materials have been explored and employed as photocatalysts for hydrogen production, most of them still suffer from a quite low photocatalytic activity, far below the requirements of practical applications. Apart from the light absorption, charge separation and transport are fundamentally important for the photocatalytic hydrogen-generation reaction. Nevertheless, the relatively inefficient separation and transfer for photoexcited electrons and holes are regarded as unavoidable deactivation processes inside the photocatalyst, which tremendously hampers the catalytic activity of the semiconductors.[3] Thus, to maximize the hydrogen generation efficiency of the photocatalyst system, the consumption of the photoexcited electrons should be avoided as far as possible during the photocatalytic process.

Elemental doping is one of the most effective approaches to regulate the electronic structure and improve the photocatalytic activity.[4] So far, in spite of research on the optimization of the photocatalytic activity by means of elemental doping in semiconductors, there still exists controversy on the role that the dopants play in photocatalysis, because dopants would act as the recombination centers for the photoexcited electrons and holes, impeding further improvement of the photocatalytic activity.[5] More importantly, for the bulk system, the external dopants tend to be randomly located in the interior of photocatalysts, which increases the recombination probability of photoexcited electrons and holes. To this end, ultrathin two-dimensional (2D) materials would provide a favorable platform to realize surface elemental doping, which could serve as an ideal model with clear structure–property relationship to achieve in-depth atomic-level insights into the correlation between the doping atoms and the corresponding photocatalytic activity.[6] Recently, $ZnIn_2S_4$ (ZIS) with a layered structure has been regarded as an excellent photocatalyst for hydrogen evolution, mainly because of its high activity, favorable chemical stability, and appropriate band gap corresponding to the visible-light absorption.[7] Notably, with its thickness reduced to only a few layers, a large proportion of interior sulfur atoms in ZIS were exposed on the surfaces, which could be readily substituted by oxygen atoms under appropriate conditions, realizing surface oxygen-doped ZIS (O-doped ZIS) nanosheets. Accordingly, the ultrathin O-doped ZIS nanosheets will provide an ideal catalytic model for understanding the role that the dopants play in the photocatalytic process.

Herein, we first use models of the ZIS ultrathin nanosheet and its oxygen-doped counterpart with only a few layers as examples to illustrate the aforementioned considerations. Density functional theory (DFT) calculations were carried out to study the effect of oxygen doping on the electronic structure of ZIS nanosheets. As shown in Figure 1 a,b, upon the substitution of oxygen for lattice sulfur atoms in ZIS nanosheets, the calculated density of states (DOS) of the O-doped ZIS exhibit a clearly increased DOS at valence band maximum (VBM) with respect to that of the pristine ZIS, revealing the effect of oxygen doping on the electronic structure, which is further confirmed by their calculated partial charge density around the VBM in Figure 1 c,d,

[*] W. L. Yang,[+] L. Zhang,[+] Dr. J. F. Xie, Dr. X. D. Zhang, Prof. Q. Zhang, Prof. Y. Xie
Hefei National Laboratory for Physical Sciences at the Microscale, Collaborative Innovation Center of Chemistry for Energy Materials, University of Science and Technology of China
Hefei, Anhui, 230026 (P.R. China)
E-mail: zhxid@ustc.edu.cn
yxie@ustc.edu.cn
Prof. Q. H. Liu, Prof. T. Yao, Prof. S. Q. Wei
National Synchrotron Radiation Laboratory, University of Science and Technology of China
Hefei, Anhui, 230029 (P.R. China)
E-mail: yaot@ustc.edu.cn
[+] These authors contributed equally to this work.

Supporting information for this article can be found under: http://dx.doi.org/10.1002/anie.201602543.

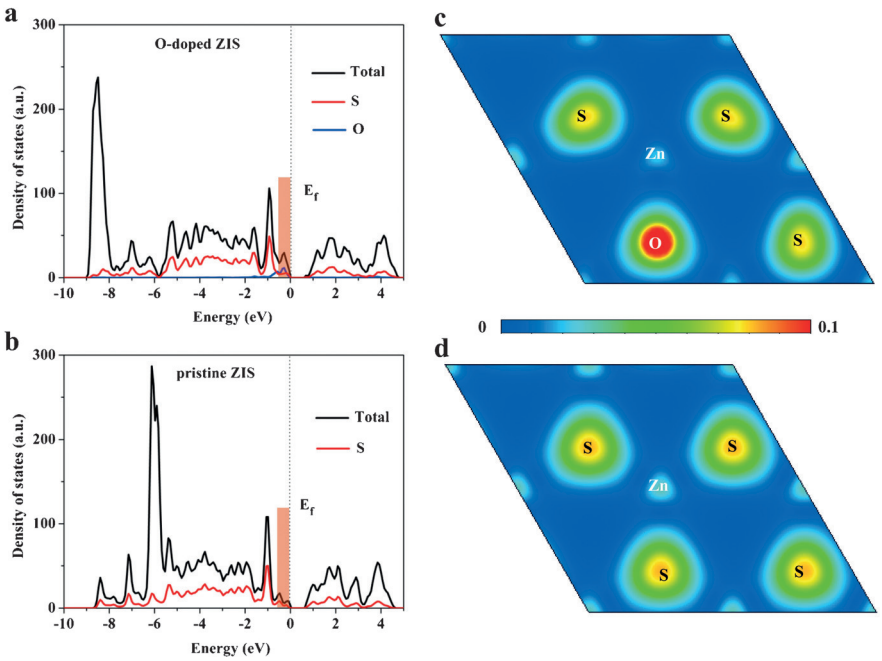

Figure 1. Calculated density of states (DOS) of a) the O-doped ZIS slab and b) pristine ZIS slab. E_f = Fermi level. The orange shading marks the increased DOS at valence-band maximum (VBM) after oxygen doping. The corresponding charge density distributions around the VBM of c) the O-doped ZIS slab and d) pristine ZIS slab, plotted from 0 (blue) to 0.1 e Å^{-3} (red).

respectively. In this case, the charge density is mainly derived from the S atoms for both the O-doped ZIS and pristine ZIS. Owing to the introduction of oxygen atoms, the O-doped ZIS has a distinctly increased charge density around the VBM in contrast to the pristine ZIS, indicating that the O-doped ZIS nanosheets could give rise to many more charge carriers that can participate in the catalytic reaction directly, which helps to significantly improve their photocatalytic performances.[8]

O-doped ZIS nanosheets were then prepared through an accessible hydrothermal synthesis process (see details in the Supporting Information). The products were recollected into powders for X-ray diffraction (XRD). As shown in Figure 2b, all the diffraction peaks could be indexed to the hexagonal phase of $ZnIn_2S_4$ without any impurity (JCPDS card No. 72-0773, $a = 3.85$ Å, $c = 24.68$ Å), indicating that the as-obtained O-doped ZIS nanosheets retain its pristine crystal structure. The morphology of the as-obtained product was studied by transmission electron microscopy (TEM) (Figure 2c), from which the nanosheets with sizes ranging from one hundred to several hundreds of nanometers can be observed. Atomic force microscopy (AFM) was performed to survey the thickness of the nanosheets. As shown in Figure 2e,f, the as-obtained product has a thickness of about 6 nm, which corresponds to five Zn-In-S molecular layers. The structure of the as-obtained nanosheets was further studied by high-resolution transmission electron microscopy (HRTEM) image on a typical nanosheet (Figure 2d). It is interesting that the HRTEM image shows discontinued crystal fringes (indicated by the dotted circles in Figure 2d) with interlayer distance of about 3.3 Å, corresponding to the (100) plane of ZIS structure, indicating the presence of large amount structure distortion in the O-doped ZIS nanosheets. In comparison, the crystal fringes of the pristine ZIS sample are intact and continued without distortion (Figure S3).

Furthermore, the chemical state and surface compositions of the O-doped ZIS nanosheets were investigated by X-ray photoelectron spectroscopy (XPS). As shown in Figure 3a, the peaks located at 531.2 and 532.0 eV can be assigned to the signal of hydroxy group and adsorbed water, respectively. Compared with pristine ZIS, the O-doped ZIS shows a new peak located at 530.0 eV, which is in agreement with the binding energy of O^{2-} ions in the metal oxide, revealing the existence of lattice oxygen in the as-prepared product.[9] And the content of lattice oxygen is estimated to be about 4.4% in the O-doped ZIS from the XPS characterization. The presence of elemental doping in the as-obtained product could be further confirmed by the photoluminescence (PL) spectra.[10] As displayed in Figure 3b, the O-doped ZIS shows a strong PL emission at about 570 nm, while the pristine ZIS shows negligible PL emission, indicating the presence of large amount defects in O-doped ZIS nanosheets. The X-ray absorption fine structure spectroscopy (XAFS) at Zn K-edge was performed to further reveal the local atomic structures of the as-obtained O-doped ZIS sample, and the results together with the ZnO data as well as the calculated spectra of ZIS are shown in Figure 3c,d. It can be found that the Zn K-edge oscillation curve for the O-doped ZIS nanosheets displays remarkable differences in comparison with the calculated spectra for bulk counterpart, implying the different local atomic arrangements of the nanosheets (Figure S7 and Table S2). Moreover, the Fourier transformed curve of O-doped ZIS nanosheets shows not only the nearest Zn–S coordination with a main peak at 1.90 Å, but also a new weak peak at about 1.39 Å. Considering the synthetic process and comparing with the FT curve of ZnO, the 1.39 Å peak can only be assigned to the Zn-O coordination. This provides strong evidences for the substitution of oxygen atoms for sulfur at the surface of ZIS. The absence of Zn–Zn coordination peak at 3.54 Å for the O-doped ZIS nanosheets can be attributed to the high structural distortion by the oxygen doping. The above results clearly indicate that the substitutional doping of oxygen in ZIS nanosheets with ultrathin thickness and structural distortions were obtained.

As an effective tool to study the electron dynamics involved in photocatalysis, ultrafast transient absorption (TA) spectroscopy can provide a direct evidence for the effect of elemental doping on the charge separation inside the semiconductors.[6,11] In the TA measurements, we adopted a femtosecond UV pump/white-light continuum (WLC) probe scheme (see details in Supporting Information). The pump

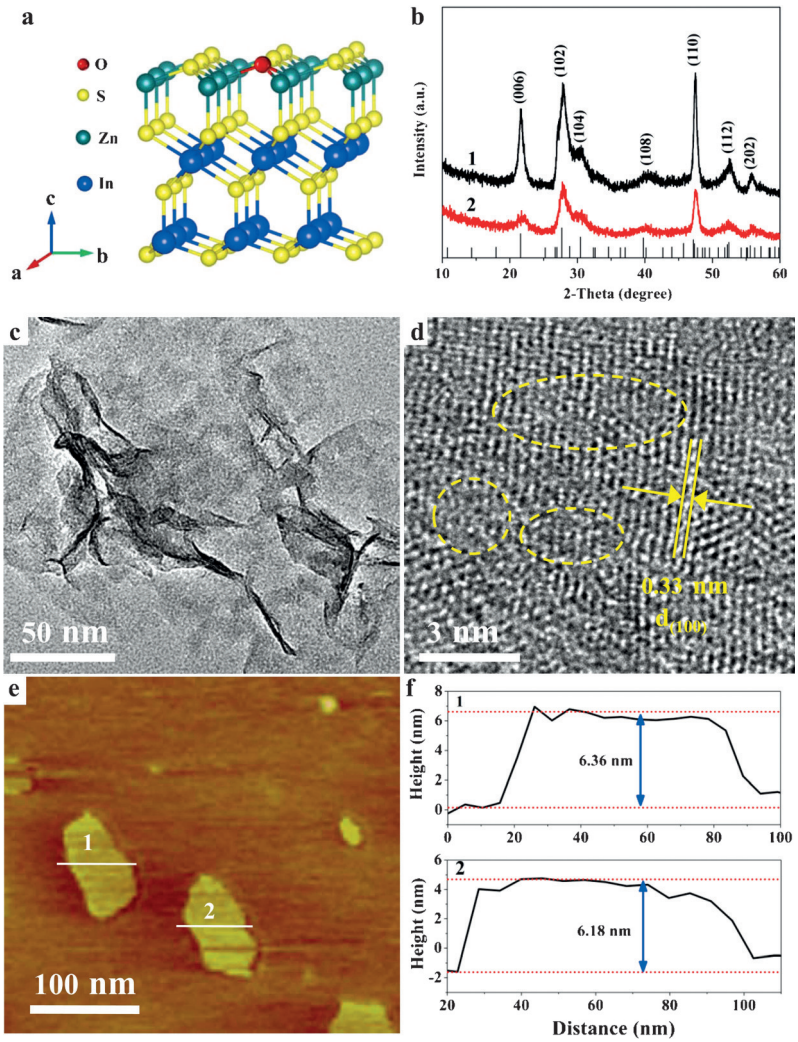

Figure 2. a) The structural model of O-doped ZIS nanosheets (Zn green, In blue, S yellow, O red). b) XRD patterns of the pristine ZIS nanosheets (1) and O-doped ZIS nanosheets (2). c) TEM image, d) HRTEM image, top view, e) AFM image, and f) the corresponding height profiles of lines 1 and 2 in (e), of the O-doped ZIS nanosheets.

was set at 400 nm, a wavelength suitable for effectively photoinducing an interband transition in the ZIS system. We show a set of representative data obtained at 690 nm, because the 610–780 nm WLC probe turned out to yield essentially the same TA kinetics for each sample. Notably, the TA kinetics for ZIS has been altered after oxygen doping. In Figure 4a, the pristine ZIS nanosheets exhibit a stimulated emission (SE) signal, which can be characterized by two time constants: $\tau_1 = 4.0 \pm 0.4$ ps (85%) and $\tau_2 = 87 \pm 16$ ps (15%), and the weighted average lifetime is 72 ± 13 ps. The O-doped ZIS nanosheets display photoinduced absorption (PA) signals as shown in Figure 4b, which can also be characterized by two time constants: $\tau_1 = 4.9 \pm 0.3$ ps (79%) and $\tau_2 = 125 \pm 12$ ps (21%), and the weighted average lifetime is 110 ± 10 ps. It should be noted that the average recovery lifetime is considered as an important parameter to evaluate the efficacy of the separation and transfer of photoexcited carriers in the photocatalytic system. Therefore, the average recovery lifetime for O-doped ZIS nanosheets is estimated to be approximately 110 ps, which is roughly 1.53 times longer than that of the pristine ZIS nanosheets (ca. 72 ps), indicating that the oxygen doping in ZIS can result in significant improvement in the electron–hole separation efficiency. On the basis of the representative observations from TA kinetics, such a lifetime increase is mainly attributed to the presence of new defect states originated from the lattice oxygen, responsible for the appearance of the new photoinduced absorption signal. In particular, after the photoexcited carriers are created in the O-doped ZIS system, the photoexcited electrons tend to be captured by the new trap states, thus dramatically promoting the separation of the photoexcited carriers, as the new trap states can offer more opportunities for photoexcited electrons to participate in the hydrogen-evolution reaction.

To verify the above expectation and shed light on the role that oxygen doping plays in the photocatalytic process, the hydrogen-evolution activity of both O-doped ZIS and pristine ZIS samples was measured in aqueous solution containing 0.25 M Na_2SO_3 and 0.35 M Na_2S under visible-light irradiation ($\lambda > 420$ nm) by a 300 W Xe lamp without adding any cocatalysts. As depicted in Figure 4c, the average hydrogen-evolution rate of the O-doped ZIS is up to 2120 $\mu mol\,h^{-1}\cdot g^{-1}$, which is 4.5 times higher than that of the pristine ZIS of 471 $\mu mol\,h^{-1}\cdot g^{-1}$, indicating the enhanced catalytic activity of the O-doped ZIS nanosheets. Furthermore, the photocatalytic activity of the O-doped ZIS nanosheets is very stable, showing negligible drops in hydrogen production rate even after twelve consecutive cycles with accumulatively 60 h under visible light irradiation (Figure 4c and S10). In addition, the hydrogen generation activity of the O-doped ZIS nanosheets matches well with its optical absorption spectrum in Figure 4d, clearly revealing that the hydrogen is primarily generated by a photocatalysis process.[12]

It has been well accepted that elemental doping can strongly influence the band structure of semiconductors, which further affect their photocatalytic activity. The band gap of the O-doped ZIS is calculated to be about 2.07 eV, which is slightly smaller than that of pristine ZIS (2.17 eV), revealing a red-shift absorption edge of ZIS upon oxygen doping. The relative locations of valence band (VB) maximum for both the O-doped and pristine ZIS were measured via the XPS valence spectra. As displayed in Figure 5c, the pristine ZIS and O-doped ZIS have distinct valence bands (VBs) with the edge of maximum energy at about 1.69 and 0.73 eV, respectively. Therefore, according to the band gap, the conduction band (CB) minimum of the O-doped ZIS upshifts by about 0.86 eV with respect to that of the pristine ZIS, as schematically illustrated in Figure 5d. On the basis of the above results, the O-doped ZIS has an increased VB width

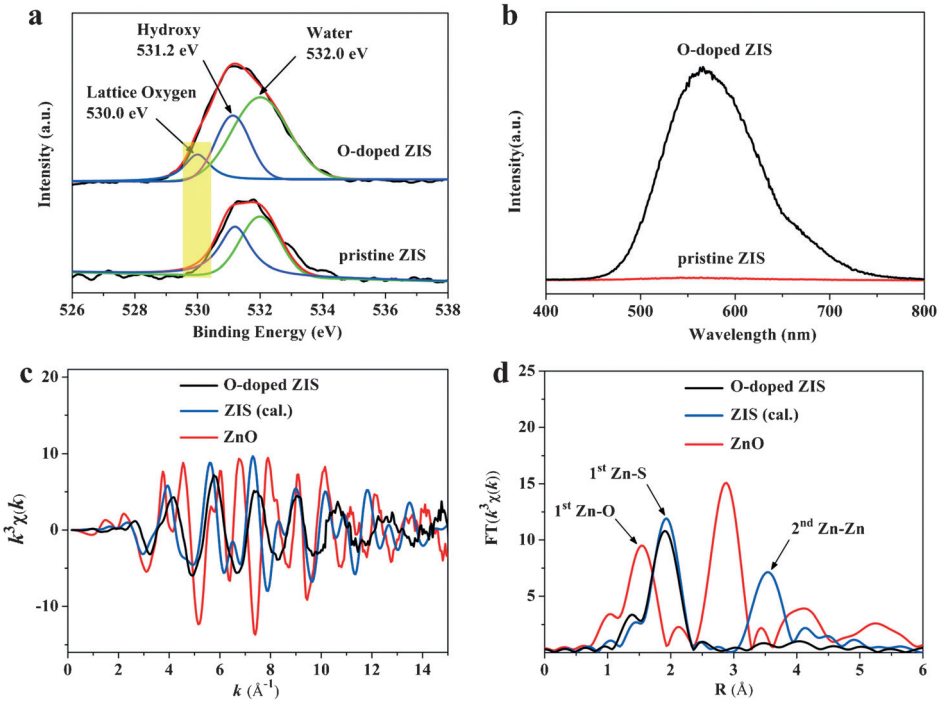

Figure 3. a) O 1s XPS spectra, yellow shading highlights new peak at 530.0 eV. b) photoluminescence (PL) spectra (excited at 365 nm) of the O-doped ZIS nanosheets and pristine ZIS nanosheets. c) Zn K-edge extended EXAFS oscillation function and d) the corresponding Fourier transforms of the O-doped ZIS nanosheets, the calculated ZIS and ZnO.

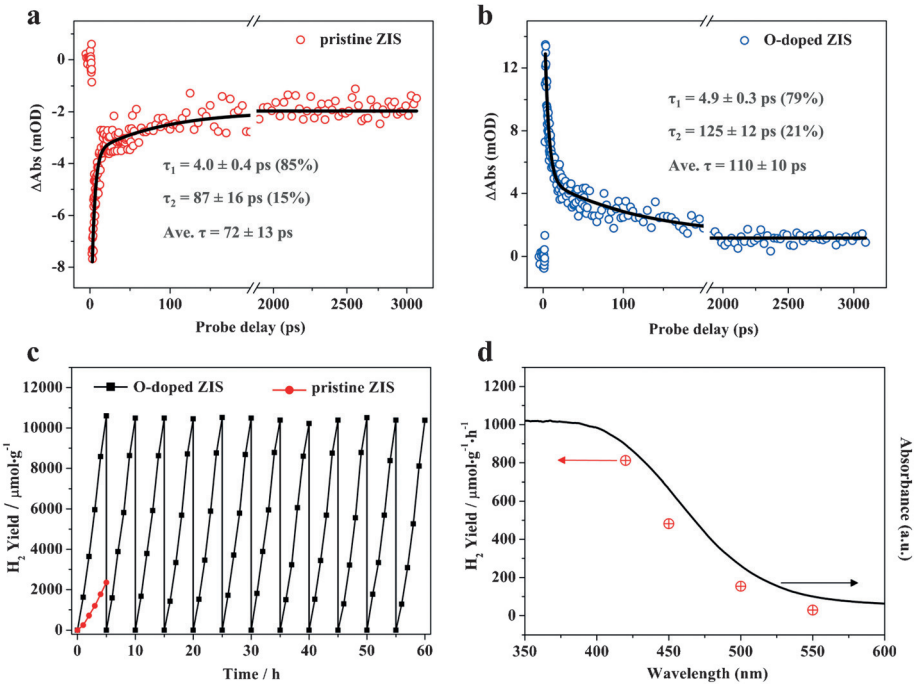

Figure 4. Ultrafast transient absorption (TA) spectroscopy of a) pristine ZIS nanosheets and b) O-doped ZIS nanosheets. The TA kinetics shown were probed at 690 nm (pump at 400 nm). The TA signal (i.e., the absorbance changes, or ΔAbs. in short) is given in mOD, where OD stands for optical density. c) Hydrogen-evolution rate of the O-doped ZIS nanosheets and pristine ZIS nanosheets, and cycling measurements for the O-doped ZIS nanosheets. d) Wavelength-dependent hydrogen-evolution activity with the O-doped ZIS nanosheets under monochromatic light irradiation. Reaction conditions: catalyst (20 mg), aqueous solution containing 0.25 M Na_2SO_3 and 0.35 M Na_2S; 300 W Xe lamp with a 420 nm cut filter.

and elevated CB minimum in contrast to the pristine ZIS, suggesting a much higher mobility and better consumption of photoexcited holes for the O-doped ZIS. On the other hand, the elevation of the CB minimum endows the photoexcited electrons in O-doped ZIS with a higher reduction ability to react with the hydrogen ions to form molecular hydrogen in the photocatalytic process compared with pristine ZIS.[13] Both the two favorable features of the energy-band structure are beneficial for inhibiting the rapid recombination of photoexcited electron–hole pairs, which is responsible for the enhanced photocatalytic performance of the O-doped ZIS sample.

In summary, we have presented the structurally new, cocatalyst-free, O-doped ZIS ultrathin nanosheet as an excellent platform to promote the photocatalytic activity through facilitating photoexcited charge-carrier separation in the photocatalytic process. The ultrathin O-doped ZIS nanosheets showed increased DOS at valence-band maximum with respect to that of the pristine ZIS sample, guaranteeing more charge carriers in photocatalysis. Furthermore, ultrafast transient absorption spectroscopy disclosed that the O-doped ZIS sample had an increased average recovery lifetime, which is roughly 1.53 times longer than that of the pristine ZIS sample, indicating a significant improvement in the separation efficiency of photoexcited carriers by doping oxygen into the ZIS crystal. As a result, the O-doped ZIS nanosheets exhibited a stable and remarkably enhanced photocatalytic activity with a hydrogen-evolution rate of up to 2120 $\mu mol\,h^{-1}\cdot g^{-1}$, which is 4.5 times higher than that of the pristine ZIS nanosheets. This work not only provides a feasible plan for the design of high-efficiency photocatalysts with stable performance through simple ele-

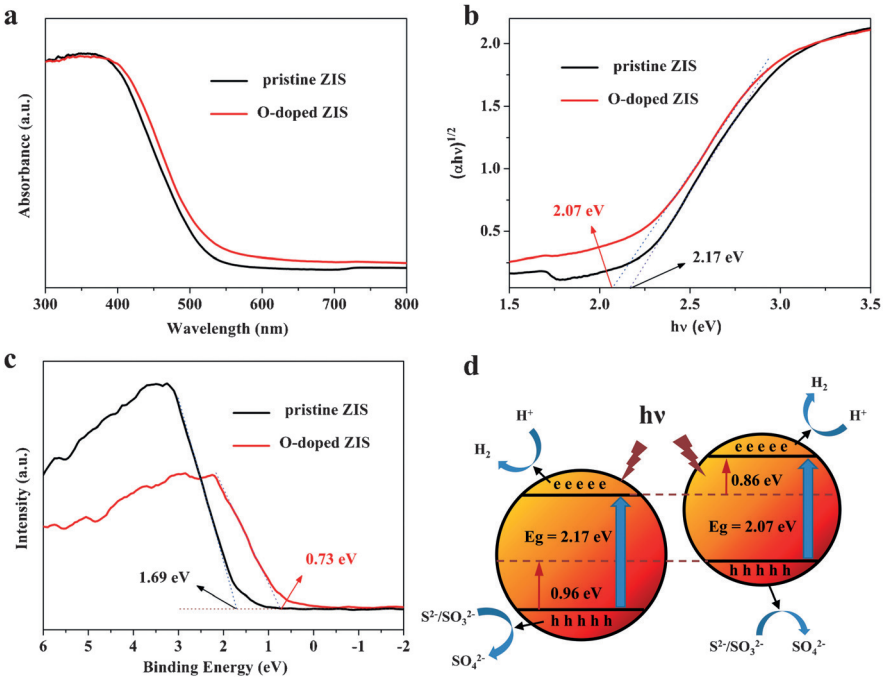

Figure 5. The contrast of a) UV/Vis absorption spectra, b) band gap that estimated by a related curve of $(\alpha h\nu)^{1/2}$ versus photon energy plotted, and c) valence-band (VB) XPS spectra of the O-doped ZIS nanosheets and pristine ZIS nanosheets. d) Schematic illustration of the band structure of the O-doped ZIS and pristine ZIS samples. h = hole.

mental doping, but also sheds light on the crucial role of elemental doping in photocatalysis at the atomic level.

Acknowledgements

The work was supported by the National Basic Research Program of China (2015CB932302), National Natural Science Foundation of China (U153226, 21331005, 11321503, 21401181, 91422303, 21573211, 11422547, 21471143), the Strategic Priority Research Program of the CAS (XDB01020000), Fundamental Research Funds for the Central Universities (WK2060190027, WK2340000063, WK2310000050), the Key Laboratory of Neutron Physics (CAEP, 2014DB01), and Research Grant of the Hefei Science Center of CAS (2015HSC-UE006, 2015HSC-UP015).

Keywords: charge-carrier separation · hydrogen evolution · oxygen doping · photocatalysis · ultrathin nanosheets

How to cite: *Angew. Chem. Int. Ed.* **2016**, *55*, 6716–6720
Angew. Chem. **2016**, *128*, 6828–6832

[1] a) A. Fujishima, K. Honda, K. Kohayakawa, *Nature* **1972**, *238*, 37–38; b) K. Maeda, K. Teramura, D. L. Lu, T. Takata, N. Saito, Y. Inoue, K. Domen, *Nature* **2006**, *440*, 295.

[2] a) X. B. Chen, L. Liu, P. Y. Yu, S. S. Mao, *Science* **2011**, *331*, 746–750; b) J. Zhang, Q. Xu, Z. C. Feng, M. J. Li, C. Li, *Angew. Chem. Int. Ed.* **2008**, *47*, 1766–1769; *Angew. Chem.* **2008**, *120*, 1790–1793.

[3] a) X. B. Chen, S. H. Shen, L. J. Guo, S. S. Mao, *Chem. Rev.* **2010**, *110*, 6503–6570; b) J. H. Huang, Q. C. Shang, Y. Y. Huang, F. M. Tang, Q. Zhang, Q. H. Liu, S. Jiang, F. C. Hu, W. Liu, Y. Luo, T. Yao, Y. Jiang, Z. Y. Pan, Z. H. Sun, S. Q. Wei, *Angew. Chem. Int. Ed.* **2016**, *55*, 2137–2141; *Angew. Chem.* **2016**, *128*, 2177–2181.

[4] a) R. Asahi, T. Morikawa, T. Ohwaki, K. Aoki, Y. Taga, *Science* **2001**, *293*, 269–271; b) C. Y. Yang, Z. Wang, T. Q. Lin, H. Yin, X. J. Lu, D. Y. Wan, T. Xu, C. Zheng, J. H. Lin, F. Q. Huang, X. M. Xie, M. H. Jiang, *J. Am. Chem. Soc.* **2013**, *135*, 17831–17838.

[5] a) X. B. Chen, S. S. Mao, *Chem. Rev.* **2007**, *107*, 2891–2959; b) C. Z. Wang, Z. Chen, H. B. Jin, C. B. Cao, J. B. Li, Z. T. Mi, *J. Mater. Chem. A* **2014**, *2*, 17820–17827.

[6] F. C. Lei, L. Zhang, Y. F. Sun, L. Liang, K. T. Liu, J. Q. Xu, Q. Zhang, B. C. Pan, Y. Luo, Y. Xie, *Angew. Chem. Int. Ed.* **2015**, *54*, 9266–9270; *Angew. Chem.* **2015**, *127*, 9398–9402.

[7] a) Z. B. Lei, W. S. You, M. Y. Liu, G. H. Zhou, T. Takata, M. Hara, K. Domen, C. Li, *Chem. Commun.* **2003**, 2143; b) B. Xu, P. L. He, H. L. Liu, P. P. Wang, G. Zhou, X. Wang, *Angew. Chem. Int. Ed.* **2014**, *53*, 2339–2343; *Angew. Chem.* **2014**, *126*, 2371–2375.

[8] X. D. Zhang, X. Xie, H. Wang, J. J. Zhang, B. C. Pan, Y. Xie, *J. Am. Chem. Soc.* **2013**, *135*, 18–21.

[9] a) R. Al-Gaashani, S. Radimana, A. R. Dauda, N. Tabet, Y. Al-Douri, *Ceram. Int.* **2013**, *39*, 2283–2292; b) J. Pfrommer, M. Lublow, A. Azarpira, C. Göbel, M. Lücke, A. Steigert, M. Pogrzeba, P. W. Menezes, A. Fischer, T. Schedel-Niedrig, M. Driess, *Angew. Chem. Int. Ed.* **2014**, *53*, 5183–5187; *Angew. Chem.* **2014**, *126*, 5283–5287; c) J. F. Xie, J. J. Zhang, S. Li, F. Grote, X. D. Zhang, H. Zhang, R. X. Wang, Y. Lei, B. C. Pan, Y. Xie, *J. Am. Chem. Soc.* **2013**, *135*, 17881–17888.

[10] S. H. Shen, L. Zhao, Z. H. Zhou, L. J. Guo, *J. Phys. Chem. C* **2008**, *112*, 16148–16155.

[11] a) L. L. Wang, J. Ge, A. L. Wang, M. S. Deng, X. J. Wang, S. Bai, R. Li, J. Jiang, Q. Zhang, Y. Luo, Y. J. Xiong, *Angew. Chem. Int. Ed.* **2014**, *53*, 5107–5111; *Angew. Chem.* **2014**, *126*, 5207–5211; b) H. Q. Xu, J. H. Hu, D. K. Wang, Z. H. Li, Q. Zhang, Y. Luo, S. H. Yu, H. L. Jiang, *J. Am. Chem. Soc.* **2015**, *137*, 13440–13443.

[12] Y. Y. Kang, Y. Q. Yang, L. C. Yin, X. D. Kang, G. Liu, H. M. Cheng, *Adv. Mater.* **2015**, *27*, 4572–4577.

[13] G. Liu, P. Niu, C. H. Sun, S. C. Smith, Z. G. Chen, G. Q. Lu, H. M. Cheng, *J. Am. Chem. Soc.* **2010**, *132*, 11642–11648.

Received: March 12, 2016
Published online: April 21, 2016